




Integration of Machine Learning (ML) and Finite Element Analysis (FEA) for Predicting the Failure Modes of a Small Horizontal Composite Blade

Ahmed Ali Farhan Ogaili ^{*,**†} , Mohsin Noori Hamzah ^{*} , Alaa AbdulhadyJaber ^{*} 

* Mechanical Engineering Department, University of Technology- Iraq/Baghdad

** Mechanical Engineering Department, University of Mustansiriyah -Iraq/Baghdad

1. (ahmed_ogaili@uomustansiriyah.edu.iq, mohsin.n.hamzah@uotechnology.edu.iq, alaa.a.jaber@uotechnology.edu.iq)

† Corresponding author; Ahmed Ali Farhan Ogaili, Tel: +9647702833351

ahmed_ogaili@uomustansiriyah.edu.iq

Received: 23.08.2022 Accepted: 06.10.2022

Abstract- This article aims to integrate machine learning (ML) methodologies and Finite Element Analysis (FEA) to analyze wind turbine blades made of composite material. The methods for wind speed forecasting were examined in this article. A suitable technique was employed for creating synthetic wind speed over four years in Baghdad, Iraq, and applied to structural analysis. Composite materials were considered to simulate a small horizontal-axis wind turbine blade. Baghdad's long-term wind speed pattern was established after the machine learning forecasting models based on autoregressive integrated moving averages (ARIMA). This wind forecast prediction was then used to mimic the dynamic loads acting on the blade. The structural behavior of a wind turbine under various loads was modeled using ABAQUS software employing three composite wind blades with varied stacking sequences. Hashin's criterion determined the structure's failure modes and most vulnerable areas. The main objectives are identifying an integrated methodology requiring high accuracy in blade modeling and wind forecasting. Damage analysis has been developed for small horizontal-axis wind turbine blades to evaluate the optimum stacking sequences of composite materials.

Keywords Failure analysis, Fault detection, composite materials, FEA, Hashin's criterion

1. Introduction

Wind energy resources are one of the most rapidly expanding hi-technologies in the energy area since they are a renewable, green, and environmentally friendly source of electricity. It is well recognized that the rotor blades of wind turbines are the most crucial component of the entire wind turbine system [1-2]. Composite materials are widely used in fabricating wind turbine blades because of their unique properties, including high specific stiffness and specific strength, better designability, high anti-fatigue, and anti-failure performance, ease of integral molding large-area parts, and excellent corrosion resistance. The development of

immense power, low weight, and high-performance ratio wind turbine blades have resulted in large-scale wind turbine blades mainly built of reinforced material and thermosetting base resin. They were now produced using a layup process [3]. However, wind speed prediction is essential to the development of wind power generation as well as the design of power equipment such as turbines. Because wind speed is a variable that changes randomly, researchers are concentrating their efforts on constructing more robust statistical models that can rapidly handle vast volumes of environmental data and accurately anticipate wind speed patterns. Smith et al. [4] pointed out that this helps in properly expecting wind generation and reduces the facility's cost. The design of wind

turbine blades is also impacted by the precision with which wind parameter predictions can be made. According to [5-6], dynamic stall, wind turbulence, and unstable aerodynamic effects are caused by unexpected and nonlinear wind speed, which affects how much useful time the wind turbine blades have left. There has been extensive study done on the dynamic analysis of wind turbine blades. Important topics like aeroelastic analysis, stability and flutter, fatigue analysis, transient analysis, and delamination growth studies have received much attention throughout time [7].

The construction of wind turbine blades (WTBs) was concentrated on the that the wind's kinetic Energy may be recovered and transformed into mechanical Energy, which can then be turned into electrical power with the assistance of a generator. WTBs experience a variety of aerodynamic, centrifugal, and gravitational loads while in use, which causes the moving rotor to experience significant fatigue stresses, especially at the blade transition zone [8]. For offshore wind turbine blades, endurance and rigidity are essential, given the upkeep requirements for renewable marine energies.

Within this framework, the development of wind energy conversion technologies will rely mainly on composite materials [9]. Because of their superior mechanical properties, composite materials were used in various applications, including Energy, aeronautics, and automotive. However, a lack of understanding of composite materials' impact and fatigue characteristics causes the structure to be overdimensioned, resulting in increased manufacturing costs [10-12]. WTBs comprise glass and carbon fiber composite materials to provide strength and durability. They are constructed using adhesive bonding technology to meet their large size. However, the adhesive's thickness may impact the structural behavior. They have relatively low stiffness, which causes them to soften before displaying a visible crack. Therefore, the increased deformation can "hide" the fracture in areas that are not apparent. However, the adhesive has already been plastically distorted to the point where it can no longer prevent the crack from propagating [14]. Hu et al. [15] proposed a technique for assessing fatigue that involves modeling a random wind field, finite element stress analysis, aerodynamic analysis, and a simulation of fatigue damage. The accumulated damage to the composite blades of the wind turbine was calculated to achieve reliability-based design optimization, taking into account wind load unpredictability. Kong et al. designed, produced and evaluated a 750 kW medium-scale E-glass/epoxy composite blade. [16]. The authors devised a method for creating structures that included aerodynamic design, studying dynamic and static loads, designing and analyzing structures, and figuring out how long they would last due to wear and tear using the random load spectrum.

Recently, numerous researchers have increasingly utilized machine learning (ML) algorithms to forecast wind energy. As wind speed is considered the primary factor that causes dynamic stresses on turbine blades, more research is being done on new techniques for forecasting wind speed. As

machine learning techniques progress, artificial intelligence models like fuzzy logic and artificial neural networks (ANN) are being used more frequently.

Mehmet Yesilbudak et al. [17] developed and utilized a KNN classifier for short-term wind speed forecasting in 2-dimensional input space. The suggested method used a 2-dimensional input space to produce forecasts at 10-min intervals. Also, the same researcher with his group [18] suggested a new way to predict wind speed in the very short term using the KNN classification approach to predict wind speed parameters in n-tuples inputs and looks at how the input parameters and distance metrics affect wind speed prediction. The KNN classification model, which uses wind direction, air temperature, and atmospheric pressure as three-fold inputs, gave the worst wind speed prediction for $k = 1$ in the Minkowski distance metric.

In another research, Wang et al. [19] suggested a hybrid model for daily wind forecasting based on Bayesian model averaging and ensemble learning (BMA-EL). This model can more accurately predict wind power under varying weather conditions. Ilhami Colak and colleagues [20] focus on multi-time series and time-scale modeling in forecasting wind speed and wind power. Different statistical models are evaluated, rated, and judged over a wide range of periods. Multi-time series modeling, such as moving average (MA), weighted moving average (WMA), autoregressive moving average (ARMA), and autoregressive integrated moving average (ARIMA), were all used in multi-time series modeling.

Erdem and Shi [21] predicted wind speed and direction using four autoregressive moving averages (ARMA) methods. As a measure of prediction quality, average absolute error (MAE) is used to compare the results. The component model predicted wind direction more accurately than the conventional ARMA model. In contrast, the opposite was observed for wind speed prediction. The ARMA model was used by Chen and Folly [22] to predict wind energy and wind speed for one hour. The accuracy of this model's wind speed and power predictions is lower than that of neural networks and neuro-fuzzy inference techniques. Sfetsos employed the autoregressive integrated moving average (ARIMA) in [23] for multi-step forecasting, averaging data from 10-minute intervals and then averaging again to provide mean hourly estimates. This model's output is superior to traditional methods considering historical mean hourly wind speeds. Kavasseri and Seetharaman [24] used the fractional-ARIMA model to forecast wind power for one and two days. Model flaws were calculated and contrasted with the persistence model. ANN and ANN-based hybrid model was developed by Cadenas and Rivera [25] for long-term wind forecasting.

Another model accounts for several characteristics, including autocorrelation, non-Gaussian distribution, and diurnal non-stationarity [26] proposed two-hybrid wind speed prediction models: ARIMA-Kalman and ARIMA-ANN. Both models function well and may be applied to non-stationary wind speeds, as demonstrated by the results. Predicting wind

speed was made possible based on a hybrid model combining ANN, ARIMA, and the wavelet transform developed by De Alencar and De Mattos Affonso [27]. Therefore, it is important to utilize an integrated system that combines the power of machine learning algorithms, like ARIMA, for long-term forecasting of wind, taking into account numerous environmental parameters to calculate wind load.

The literature review on wind modeling and wind turbine blade analysis reveals that although there are numerous studies on wind prediction methods and blade structural and fatigue analyses, there are very few studies for an integrated framework beginning with long-term wind forecasting, aerodynamic and structural analyses, and fatigue analysis of composite horizontal-axis wind turbine blades with limited or no raw wind data. In other words, a system that can combine the strength of ML algorithms like ARIMA will be developed in this research. This kind of system can be used to analyze the damage caused to long wind turbine blades by employing a 3D CAD and FE model with a high accuracy level.

The unique contribution of this study is that it compares the various machine learning wind forecasting models to select the best suitable for damage analysis applications. It develops long-term wind profile predictions for sites that do not have enough historical wind measurement data to a good level of accuracy; it performs high-fidelity three-dimensional (3D) modeling and analysis considering random wind loads for damage analysis. The main focus is on developing an integrated procedure incorporating long-term wind forecasting methods for blade damage analysis. The predicted long-term wind load is then used in the damage analysis, considering how the wind load changes at a chosen location in Baghdad, Iraq.

The article's organization is as follows: the following section discusses the source from which the wind data were obtained. Section 3 deliberates the use of machine learning techniques for predicting wind speed. Sections 4 and 5 discuss the main blade design and the composite materials used. However, the considered failure criterion is presented in Section 6. After that, the blade modeling based on FEA is discussed in Section 7, and the results are presented in Section 8. Finally, the article is wrapped up in Section 9.

2. Wind Data Source

The current study adopted the wind speed dataset from the first of January/2016 to the first of January 2022 in Baghdad city/Iraq, from the OpenWeatherMap website. This data gave us the needed information to anticipate the wind speed profile [28]. A non-stationary time series, such as the one shown in Figure 1, would typically exhibit non-stationary features such as time-varying mean and variance. Non-stationary time series information has some characteristics, such as the inability to rapidly infer the typical patterns from the signal and the need for careful attention when formulating forecasts using this data. Hence, the ARIMA

modal will be utilized for wind prediction, which will be explained further in the next section.



Fig. 1. Wind speed time series.

3. Machine Learning Approach

Machine learning is a branch of Artificial Intelligence (AI) that has grown out of pattern recognition. Machine learning (ML) is a subfield of computer science and a subdiscipline of artificial intelligence whose foundation is a set of statistical methods that focus on building predictive models using learning and training data. Widespread applications of machine learning techniques have previously been adopted to forecast wind speed distribution [29-30]. Due to their capacity to manage various variables through self-improvement without explicit instructions [31-32], machine learning models have attracted considerable interest. These algorithms are divided into four major classes: supervised learning, unsupervised learning, semi-supervised learning, and reinforcement learning. The most extensively used algorithms for prediction are supervised learning algorithms, which give a learning scheme with "labeled data" and are designed to classify fresh data sets [33].

3.1. ARIMA Modal

Autoregressive Integrated Moving Average (ARIMA) is one of the most straightforward and successful machine learning algorithms for forecasting time series; it combines autoregression and moving average steps [34]. The ARIMA technique's diagnostic control, identification, and estimation phases are divided into three steps [35]. In the first step, called diagnoses control, stationarity control is used on the time series data given. A stationary time series is one in which the mean, standard deviation, and covariance change over time. Stationarity is a prerequisite for the ARIMA model, which makes estimates accurate and helpful. Assume that the time series presented is not stationary. In this instance, the stationarity is reassessed once the requisite degree of difference (d) has been applied. Up until a consistent pattern is created, this is repeated many times. However, d is a positive number indicating the difference's magnitude. If the difference is measured d times, the model's ARIMA integration parameter is set to d . The identification technique is then applied to the

stationary data that was collected. The parameters p and q are not used in this procedure. The parameters (p) and (q) for the moving average (MA) and autoregressive (AR) transactions are discovered in this step. The ARIMA model is discussed using ARIMA parameters, which are p , d , and q [36]. Where p is the autoregressive model (AR) degree, d is the difference degree, and q lagged prediction, as shown in the following Equation:

$$y_t = \phi_1 y_{t-1} + \phi_2 y_{t-2} + \dots + \phi_p y_{t-p} + \delta + a_t - \theta_1 a_{t-1} - \theta_2 a_{t-2} \dots \theta_q a_{t-q} \tag{1}$$

y_t, y_{t-1}, y_{t-p} are d -order difference observations, $\phi_1, \phi_2, \dots, \phi_p$ are coefficients of the order difference observations, δ is the constant value, $a_t, a_{t-1}, a_{t-2}, \dots, a_{t-q}$ are error values, and $\theta_1, \theta_2, \dots, \theta_p$ are errors coefficients [37]. Here, y_t is the data that has been linearized, and a_{t-1} is the error in the moving average for time t .

To obtain the forecast data, you must first estimate $p, q,$ and d . To do this, separate the data and look for a stationary trend in the partial autocorrelation function (PACF) and autocorrelation function (ACF) plots for p and q , respectively. So, the last lag after PAC stops is used to figure out the value of p , and the last lag after ACF stops is used to figure out the value of q . After the identification phase, the estimation phase finds ϕ_p and θ_p Parameters using maximum likelihood estimation or back-casting methods. When the model is fit, the diagnostic checking on the residuals' autocorrelation plots is performed to check for any large autocorrelations. p and q are changed if they need to be. This is the last part of the diagnostic check.

3.2. Model Accuracy Evaluation

Root Mean Square Error (RMSE), Mean Absolute Percentage Error (MAPE), and Mean Absolute Error (MAE), are some of the most often utilized parameters to analyze the accuracy or certainty of the models developed for calculating wind velocity forecasts. The square root of the mean of the square of all the errors is called the root mean square error (RMSE). In both statistics and machine learning, RMSE in regression is highly popular and is regarded as a superior all-purpose error metric for numerical predictions. A larger RMSE denotes significant differences between the expected and actual values. The fact that the errors are squared, which results in a much bigger weight ascribed to larger errors, is another significant characteristic of the RMSE [37].

Consequently, an error of 10 is 100-times worse than an error of 1. The MAE is the simple mean of absolute errors. Absolute error is the difference between the predicted value and the actual value. The MAE informs us about the average magnitude of the forecast error.

They are using the MAE, and the error increases linearly. Therefore, a 10-point error is 10-times worse than a 1-point error. Since MAD is a relative measure, MAPE scales MAD to be expressed in percentage units rather than the variable's units. MAPE is a relative error metric that compares the

forecast accuracy of time-series models by utilizing relative errors to prevent positive and negative errors from canceling one another out. However, RMSE, MAE, and MAPE are determined using the following equations [38]:

$$RMSE = \sqrt{\left(\frac{1}{n} \sum_{t=1}^n (y_t - f_t)^2\right)} \tag{2}$$

$$MAE = \frac{1}{n} \sum_{t=1}^n |y_t - f_t| \tag{3}$$

$$MAPE = \frac{1}{n} \sum_{t=1}^n \left| \frac{y_t - f_t}{y_t} \right| \tag{4}$$

Where n is the number of errors, y_i is the actual value, and f_t is the forecasted value. As seen in Equation (2), the primary objective of MAPE is to demonstrate whether or not the data are stable (i.e., whether or not the variance is significant). For this reason, MAPE is substantial in wind power prediction. It shows that RMSE is a quadratic scoring rule [38]. Forecast differences are squared, added, and averaged over the sample size. Then, the average square root is calculated.

Akaike Information Criterion (AIC) is an information criterion commonly used for model selection. Also, the Bayesian Information Criterion (BIC) is a common criterion for choosing ARIMA-based models [39].

The wind speed data set was used as training data for building the ARIMA model. The Orange software was employed to build the ARIMA model to determine the wind's autocorrelation and partial autocorrelation plots. As shown in Table 1, the AR, MA, and integration parameters were discovered to be of the ARIMA (1,1,2) series using the Orange software function "estimate," which has lowermost AIC and BIC values when compared to the other trials. When choosing an ARIMA-based model, AIC and BIC criteria are often used. The parameters of the ARIMA (1,1,2) model are shown in Table 1, illustrating how well it matches the data. Figure2 depicts the ARIMA wind speed prediction for the upcoming five years.

Table 1. ARIMA models' comparison.

ARIMA (p,d,q)	RMSE	MAE	MAPE	R ²	AIC	BIC
ARIMA(1,0,0)	1.25	0.71	0.282	0.225	204.7	211
ARIMA(1,1,1)	1.297	0.797	0.293	0.198	206.8	215.1
ARIMA(1,1,2)	1.209	0.806	0.279	0.303	201	211.4
ARIMA(2,1,1)	1.295	0.897	0.291	0.201	208.5	218.8
ARIMA(2,1,2)	1.251	0.885	0.291	0.254	206.8	219.3
ARIMA(2,1,3)	1.203	0.823	0.278	0.31	204.6	219.2

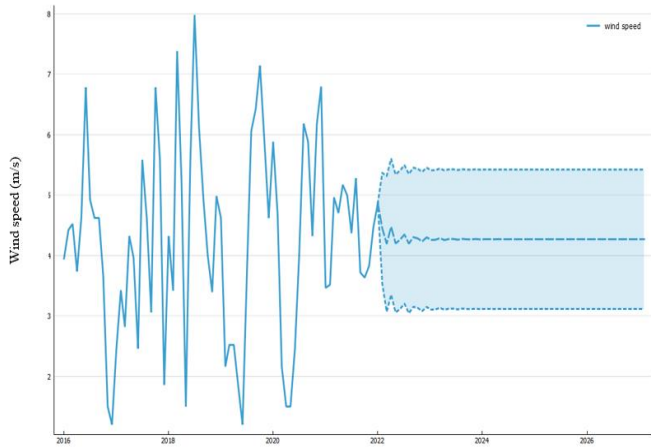


Fig.2. Wind speed forecasting by ARIMA

4. Blade Structure and Design

The most critical part of an Airfoil is the material of choice when constructing wind turbine blades, as the whole blade consists of airfoil sections. The rotation of the blade is caused by the lift created by this airfoil at each segment. The airfoil shape of the blade was generated using the Blade Element Momentum (BEM) theory and the Qblade program, free software dedicated to the simulation and design of wind turbines. This profile includes coordinates for the profile's points. These coordinates can create a SOLIDWORKS profile of the NACA 4412 standard. Figure (3-4). illustrates the airfoil section and the model, respectively. The model studied in this article has been considered here to develop a blade of 400 mm in length for a small horizontal axis wind turbine of 600W power output [40].

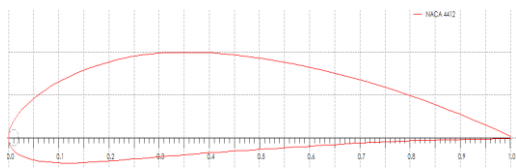


Fig.3. 4412 airfoil section

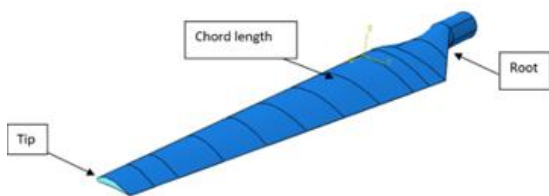


Fig.4. The WTB model

5. Blade Material

Composite materials, particularly wind Energy, provide new prospects because of their enhanced mechanical properties. Nevertheless, their behavior can be very different

because of flaws made or caused by them in service [41-44]. The bulk of wind turbine components was manufactured of GFRP (glass-fiber-reinforced polymer), which is easy to work with, does not require advanced technology reasonably priced, and has suitable elastic properties. Glass fibers have primarily replaced steel in recent years, as they are stronger and lighter. Furthermore, fatigue resistance is significantly more crucial [45-48]. However, a lack of knowledge of the behavior of composite materials causes significant extra costs related to the manufacturing of structures. The structural design demands materials with a high strength-to-weight ratio, a high stiffness-to-weight ratio, high fatigue resistance, and a low density. The purpose of this section is to evaluate the behavior of the blade when different fiber orientations are considered, such as [45/0/-45]s, [0/±45/90]s, and [0/90]s. For the remainder of this investigation, the three composites codes will be referred to as S1, S2, and S3, respectively, for [45/0/-45], [0/±45/90], and [0/90], respectively, as shown in Figure 2. The material parameters are stated in Table 2.

Table 2. Mechanical properties of the materials used in the analysis of wind turbine blades [49]

Parameter	GFRP (E-glass/Epoxy)
Density ρ (kg/m ³)	1800
Longitudinal modulus, E_{11} (GPa)	143
Transverse moduli, E_{22} (GPa)= E_{33} (GPa)	97.2
Principal Poisson's ratio, ν_{12}	0.28
Principal Poisson's ratio, $\nu_{23} = \nu_{13}$	0.23
Shear moduli, G_{12} (GPa)	3.6
Shear moduli, $G_{23} = G_{13}$ (GPa)	5.6

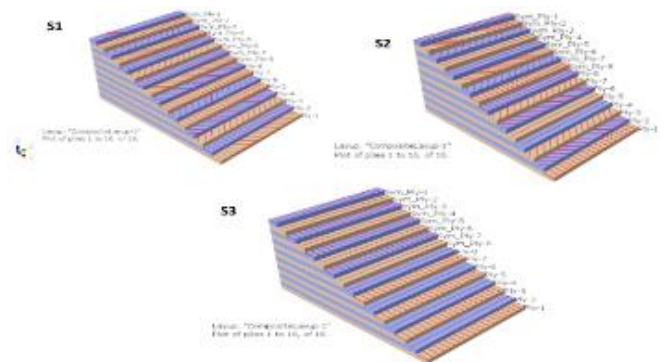


Fig. 4. The material cod of three samples in this study

6. Hashin Failure Criterion

The Hashin failure theory was used to develop a damage evaluation for glass-fiber-reinforced polymer (GFRP) composite blades. The damage behaviors were described using common failure mechanisms such as fiber tension and compression and matrix tension and compression. The occurrence of damage in a composite material is referred to as damage initiation [50]. The several failure mechanisms are examined using Hashin's criterion, which uses many constraint components. Hashin's (1980) [51] criterion's failure modes are connected to matrix and fiber failure modes. They involve four distinct damage initiation processes for composite materials: matrix failure (HSNFCCRT), fiber failure (HSNFCCRT), and fiber compression (HSNFCCRT) (HSNFCCRT). The tension between (HSNMTCRT) and (HSNMCCRT) (HSNMTCRT). According to [50], the "Hashin's criteria" for fiber-reinforced composites integrated into ABAQUS are based on Hashin. Hashin and Rotem's (1973) [50] proposed four forms of equations for failure, presented in Table 3, which are represented by $f_1, f_2, f_3,$ and f_4 . The material properties that appeared in these equations can be found in Table 2.

Table 3. Hashin's failure criteria [50]

Failure mode and condition Failure criteria	Failure mode and condition Failure criteria
Tensile fiber failure for $\sigma_{11} \geq 0, f_1 \geq 1$	$\left(\frac{\sigma_{11}}{X_T}\right)^2 + \alpha * \left(\frac{\sigma_{12}}{S_{LT}}\right)^2 = f_1$ where $0 \leq \alpha \leq 1$
Compressive fiber failure for $\sigma_{11} < 0, f_2$	$\left(\frac{\sigma_{11}}{X_C}\right)^2 = f_2$
Tensile matrix failure for $\sigma_{11} + \sigma_{33} > 0, f_3 \geq 1$	$\left(\frac{\sigma_{22}}{Y_T}\right)^2 + \left(\frac{\sigma_{12}}{S_{LT}}\right)^2 = f_3$
Compressive matrix failure for $\sigma_{22} + \sigma_{33} < 0, f_4 \geq 1$	$\left(\frac{\sigma_{22}}{2S_{TT}}\right)^2 + \left[\left(\frac{Y_C}{2S_{TT}}\right)^2 - 1\right] * \frac{\sigma_{22}}{Y_C} + \left(\frac{\sigma_{12}}{S_{LT}}\right)^2 = f_4$

In the above equations, the X_T is the longitudinal tensile strength. X_C is the compressive, tensile stress, Y_T and Y_C are the transverse tensile and compressive strength, respectively, and S_{TT} and S_{LT} represent the ply's longitudinal and transverse shear strength. $\sigma_{11}, \sigma_{22},$ and σ_{12} define the components of an effective stress tensor, and α is the contribution of shear stress to the fiber.

7. Modeling Using the Finite Element Method.

ABAQUS, an FEA software, has investigated the structure's loads, deformation, and damage initiation. The

boundary conditions of the "Encastre" type are applied to the composite blade at the root region in the investigation findings of the numerical study acquired by fixing the root of the rotor blade and leaving the tip of the rotor, where the blade is fixed where $u1 = u2 = u3 = ur1 = ur2 = ur3 = 0$, as shown in figure 3.

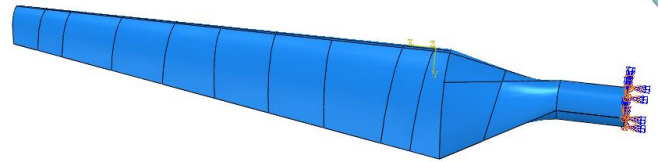


Fig. 5. The boundary condition applied to the blade

7.1. Loads Applied On the Blade

For estimation of the dynamic load applied on the blade, the predicted wind speeds obtained for five years based on the developed ARIMA model in Section 11 are utilized to compute the dynamic loads using the BEM method. According to [52-53], the flatwise and edgewise load caused by the wind is the primary source of dynamic loading on the blade that causes damage. The drag and lift forces are calculated using Equations (4) and (5), which are as follows:

$$F_{drag} = \frac{1}{2} \rho V^2 A C_d \tag{5}$$

$$F_{lift} = \frac{1}{2} \rho V^2 A C_l \tag{6}$$

$$F_{result} = \sqrt{(F_{drag})^2 + (F_{lift})^2} \tag{7}$$

$$F_c = 0.5mR\omega^2 \tag{8}$$

F_{drag} and F_{lift} are the drag and lift forces operating on the blade, as depicted in Figure 6b. V stands for wind velocity and air density, A for the rotor's swept area, and C_d and C_l for the blade profile's drag and lift coefficient (0.86 and 0.0126, respectively) for the airfoil considering the angle of attack at 4.1° and a Reynolds number of 1 million, as referred from [54]. The mass of the blade, m , equals the force of gravity, F_g , and the centrifugal force F_c , equals to $mR\omega^2$ where R is the blade span's radius and angular rotor speed. Displays the critical variables affecting the dynamic loads on the present blade. The loads applied on the blade are calculated from the above equations. And then, the pressure was estimated on the 13 blade sections and used the blade's pressure in ABAQUS finite element analysis software, as shown in Figure (6).

For validation purposes, the obtained results in this research were compared to the aerodynamic analysis used by researchers, such as [55-56] for dynamic blade load calculation. Their similarity was very close.

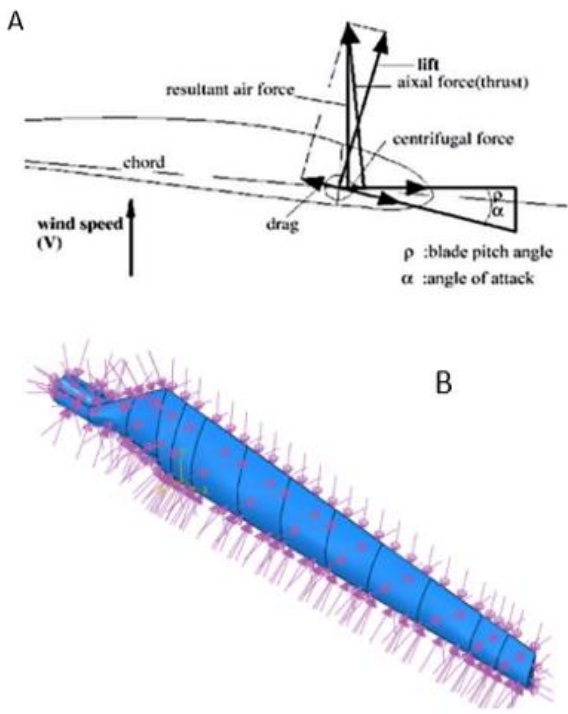


Fig. 6. A) Aerodynamic forces on the blade [52] B) Distribution of aerodynamic load

7.2. Mesh Analysis

The finite element method (FEM) is based on dividing the blade geometry into tiny domains according to the kind of mesh used to solve the problem. The higher and more precise the FEM solution, the finer the mesh size used to achieve it. The present model employs shell elements of type SC8R with a mesh size of 20 mm throughout the whole geometry. Figure 7 shows the mesh size of the blade. The shell elements provide the same level of precision as solid elements at a lower cost of calculation than solid elements. According to [57], it is better to use solid components because of their flexibility.

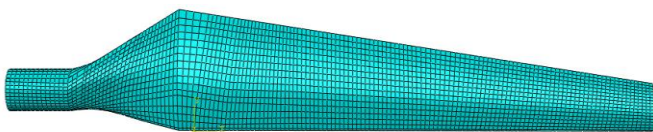


Fig. 7. The mesh of the blade

8. Results and Discussion

In this study, the Hashin failure criterion has been chosen to describe the progression of damage to the blade (occurrence). Comparing the outcomes of the three composite blades subjected to various loads, Figure (8) illustrates the fundamental displacement values that the blade with three stacking sequences of glass fibers exhibits at its tip. When comparing the findings of the two composite blades (S_2 and S_3) under the same load conditions, it is clear from Figure (8-9) that the blade (S_2) has fundamental displacement values at its tip and exhibits great resistance to damage and displacement.

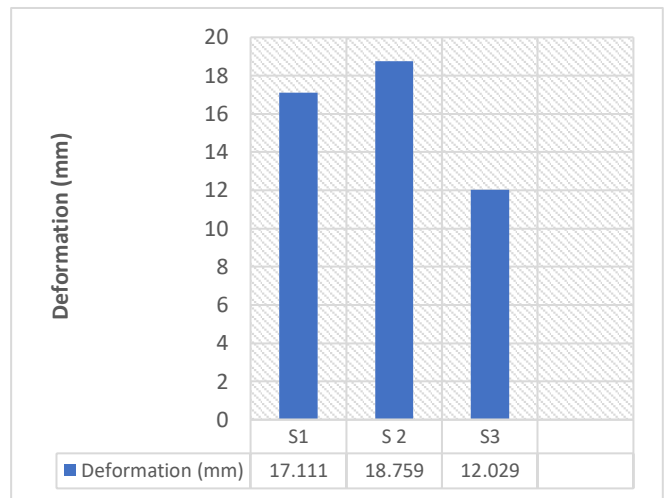


Fig. 8. Deformation of the blade tip

For Hashin's damage failure criterion result, Figures (10,11, and 12) illustrate the damage to composite blades (S_1 , S_2 , and S_3) during the same wind storm. The damage modes are localized and rely on the composite material employed and the wind speed. Each material group has equal damage. The damage values for both materials are virtually comparable at the same velocity. The model displays fiber and matrix modes damage happens in places with much stress, like near the blade's root and the level of the spars. Because of the simulation's findings, we can identify and forecast the zones susceptible to damage and failure and estimate the Influence that the stacking sequence parameters have. On a microscopic scale, the damage manifests as cracking in the matrix, disruption of the contact between the fibers and the matrix, delamination, and failure of the fibers. The internal plies around the blade's root and at the spar level are the high-stress concentration zones where the damage takes place. The investigation came to the following conclusion A thickness transition between those zones causes the damage that appears in the area of blade assembly with the hub.

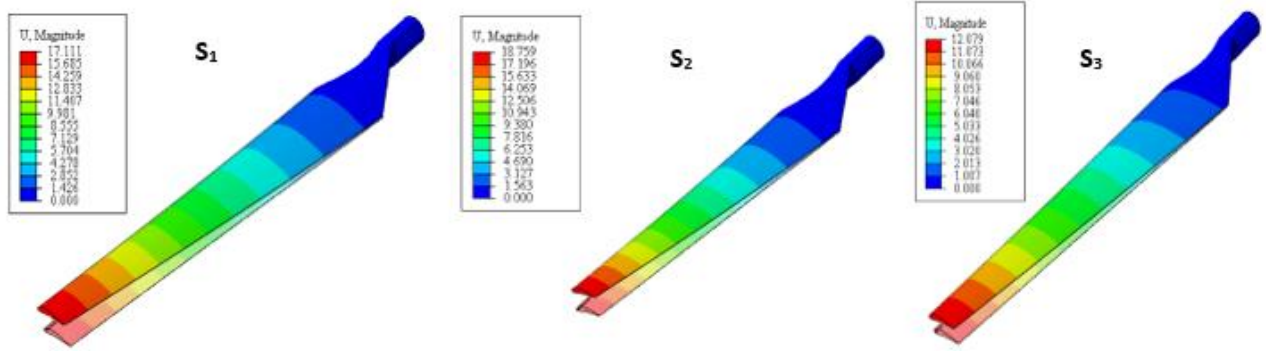


Fig. 9. Deformation at the tip of the blade (mm)

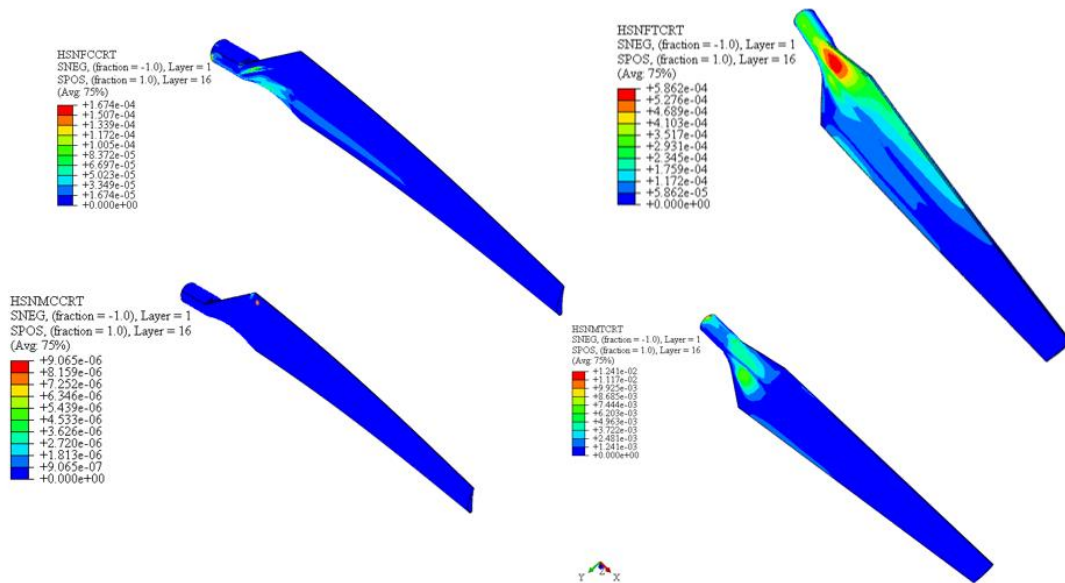


Fig.10. Hashin's damage criterion of wind turbine bladeS1

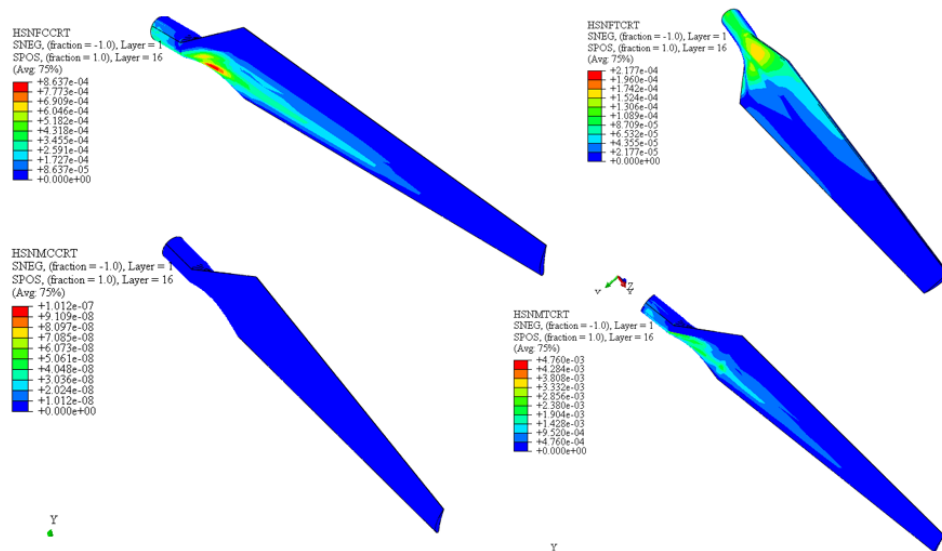


Fig.11. Hashin's damage criterion of wind turbine bladeS2

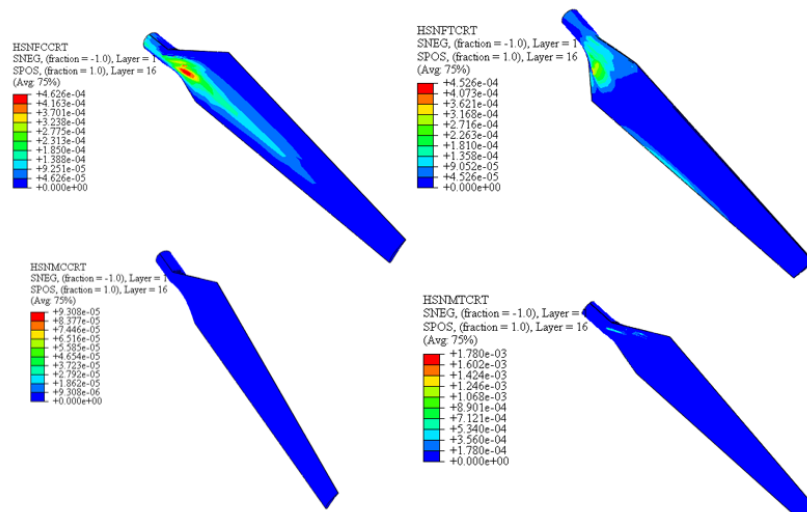


Fig.12. Hashin's damage criterion of wind turbine bladeS3

5. Conclusion

This work proves that numerical simulation may be a powerful technique for reproducing the experimental approach; it allows for predicting failure modes and identifying sensitive zones on WTBS using the finite element method. Firstly, the wind pattern for the city of Baghdad in Iraq was predicted utilizing the machine learning modal based on ARIMA using Orange software. These models were created based on the mean wind speed and Weibull distribution statistics available for Baghdad city. Accordingly, the ARIMA machine learning (ML) methodology was chosen because of its high level of precision, and the wind loads for five years were calculated for the predicted wind pattern. After the load prediction step, it is divided on the blade surface area to convert it to pressure and fed to the ABAQUS software for simulation purposes. The simulation findings enable us to detect and anticipate the vulnerable zones to damage and failure and estimate the Influence of the stacking sequence parameters. The damage occurs at the microscopic scale with matrix cracking, breaking the fibers–matrix interface, delamination, and fiber failure. The Hashin criteria for failure mode calculating results and experience are used for the three types of fiber layup systems. The optimal layup schema S_2 was determined through Hashin failure analysis of various structures.

References

- [1] C. Amer and M. Sahin, "Structural analysis of a composite wind turbine blade," *International Journal of Aerospace and Mechanical Engineering*, vol. 8, no. 7, pp. 1264-1270, 2014.
- [2] Y.Eldahab, H.Naggar H. Saad, and Abdalhalim Zekry, "Assessing Wind Energy Conversion Systems Based on Newly Developed Wind Turbine Emulator." *International Journal of Smart Grid-ijSmartGrid* ,Vol.4, pp 139-1270.
- [3] H.Boudounit, M.Tarfaoui, Dennoun Saifaoui, and Mourad Nachtane. "Structural analysis of offshore wind turbine blades using finite element method." *Wind Engineering*, Vol.44, no. 2,pp168-180.
- [4] J.Smith, Charles, Mark L. Ahlstrom, Robert M. Zavadil, Ali Sadjadpour, and C. Russell Philbrick. "The role of wind forecasting in utility system operation." In 2009 IEEE Power & Energy Society General Meeting, pp. 1-5. IEEE,26 June 2009.
- [5] Mo W, Li D, Wang X, et al. Aeroelastic coupling analysis of the flexible blade of a wind turbine. *Energy* 2015; 89: 1001–1009.
- [6] X.Liu, L. Cheng, Shi Liang, Ajit Godbole, and Yan Chen. "Influence of large-scale wind turbine blade vibration on the aerodynamic load." *Energy procedia* 75 pp.873-879,Aug 2015.
- [7] Liu X, Lu C, Liang S, et al. Vibration-induced aerodynamic loads on large horizontal axis wind turbine blades. *Appl Energy* 2017; 185: 1109–1119
- [8] X.Liu, L. Cheng, L.Shi, Ajit Godbole, and Yan Chen. "Vibration-induced aerodynamic loads on large horizontal axis wind turbine blades." *Applied Energy*, Elsevier, Vol.185, pp. 1109-1119.
- [9] M.Tarfaoui, M.Nachtane, H.Khadimallah,and D. Saifaoui. "Simulation of mechanical behavior and damage of a large composite wind turbine blade under critical loads." *Applied Composite Materials Springer*, Vol 25, no. 2, pp. 237-254.
- [10] J. N. Goundar and M. R. Ahmed, "Design of a horizontal axis tidal current turbine," *Applied energy*, vol. 111, pp. 161-174, 2013.

- [11] P. Schubel, R. Crossley, E. Boateng, and J. Hutchinson, "Review of structural health and cure monitoring techniques for large wind turbine blades," *Renewable Energy*, vol. 51, pp. 113-123, 2013.
- [12] O. R. Shah and M. Tarfaoui, "Effect of damage progression on the heat generation and final failure of a polyester-glass fiber composite under tension-tension cyclic loading," *Composites Part B: Engineering*, vol. 62, pp. 121-125, 2014.
- [13] J. Arbaoui, M. Tarfaoui, C. Bouery, and A. El Malki Alaoui, "Comparative study of mechanical properties and damage kinetics of two-and three-dimensional woven composites under high-strain rate dynamic compressive loading," *International Journal of Damage Mechanics*, vol. 25, no. 6, pp. 878-899, 2016.
- [14] S. Ke, T. Wang, Y. Ge, and Y. Tamura, "Aerodynamic loads and aeroelastic responses of large wind turbine tower-blade coupled structure in yaw condition," *Structural engineering and mechanics: An international journal*, vol. 56, no. 6, pp. 1021-1040, 2015.
- [15] W. Hu, O. I. Zhupanska, J. Buchholz, and K. K. Choi, "A new fatigue analysis procedure for composite wind turbine blades," in *32nd ASME wind energy symposium*, 2014, p. 0173.
- [16] C. Kong, J. Bang, and Y. Sugiyama, "Structural investigation of composite wind turbine blade considering various load cases and fatigue life," *Energy*, vol. 30, no. 11-12, pp. 2101-2114, 2005.
- [17] M. Yesilbudak, S. Sagiroglu, and I. Colak, "A wind speed forecasting approach based on 2-dimensional input space," in *2012 International Conference on Renewable Energy Research and Applications (ICRERA)*, 2012: IEEE, pp. 1-5.
- [18] M. Yesilbudak, S. Sagiroglu, and I. Colak, "A new approach to very short term wind speed prediction using k-nearest neighbor classification," *Energy Conversion and Management*, vol. 69, pp. 77-86, 2013.
- [19] G. Wang, R. Jia, J. Liu, and H. Zhang, "A hybrid wind power forecasting approach based on Bayesian model averaging and ensemble learning," *Renew. Energy*, vol. 145, pp. 2426-2434, 2020, doi: <https://doi.org/10.1016/j.renene.2019.07.166>.
- [20] I. Colak, S. Sagiroglu, M. Yesilbudak, E. Kabalci, and H. I. Bulbul, "Multi-time series and-time scale modeling for wind speed and wind power forecasting part I: Statistical methods, very short-term and short-term applications," in *2015 International Conference on Renewable Energy Research and Applications (ICRERA)*, 2015: IEEE, pp. 209-214.
- [21] E. Erdem and J. Shi, "ARMA based approaches for forecasting the tuple of wind speed and direction," *Applied Energy*, vol. 88, no. 4, pp. 1405-1414, 2011.
- [22] Q. Chen and K. A. Folly, "Wind Power Forecasting," *IFAC-PapersOnLine*, vol. 51, no. 28, pp. 414-419, 2018, doi: <https://doi.org/10.1016/j.ifacol.2018.11.738>.
- [23] A. Sfetsos, "A novel approach for the forecasting of mean hourly wind speed time series," *Renewable Energy*, vol. 27, no. 2, pp. 163-174, 2002.
- [24] R. G. Kavasseri and K. Seetharaman, "Day-ahead wind speed forecasting using f-ARIMA models," *Renewable Energy*, vol. 34, no. 5, pp. 1388-1393, 2009.
- [25] E. Cadenas and W. Rivera, "Wind speed forecasting in three different regions of Mexico, using a hybrid ARIMA-ANN model," *Renewable Energy*, vol. 35, no. 12, pp. 2732-2738, 2010.
- [26] H. Liu, H.-q. Tian, and Y.-f. Li, "Comparison of two new ARIMA-ANN and ARIMA-Kalman hybrid methods for wind speed prediction," *Applied Energy*, vol. 98, pp. 415-424, 2012.
- [27] D. Barbosa de Alencar, C. de Mattos Affonso, R. C. Limão de Oliveira, J. L. Moya Rodriguez, J. C. Leite, and J. C. Reston Filho, "Different models for forecasting wind power generation: Case study," *Energies*, vol. 10, no. 12, p. 1976, 2017.
- [28] Open Weather Map, <https://openweathermap.org/history-bulk>. Last access on 21/3/2022.
- [29] M. A. Wani and M. Yesilbudak, "Recognition of wind speed patterns using multi-scale subspace grids with decision trees," *International Journal of Renewable Energy Research*, vol. 3, no. 2, pp. 458-462, 2013.
- [30] G. Shobha and S. Rangaswamy, "Chapter 8 - Machine Learning," in *Computational Analysis and Understanding of Natural Languages: Principles, Methods and Applications*, vol. 38, V. N. Gudivada and C. R. B. T.-H. of S. Rao, Eds. Elsevier, 2018, pp. 197-228.
- [31] Ü. Çetinkaya, E. Avcı, and R. Bayindir, "Time series clustering analysis of energy consumption data," in *2020 9th International Conference on Renewable Energy Research and Application (ICRERA)*, 2020: IEEE, pp. 409-413.
- [32] E. H. Flaieh, F. O. Hamdoon, and A. A. Jaber, "Estimation the natural frequencies of a cracked shaft based on finite element modeling and artificial neural network," *International Journal on Advanced Science, Engineering and Information Technology*, vol. 10, no. 4, pp. 1410-1416, 2020.
- [33] T. A. Dhomad and A. Jaber, "Bearing fault diagnosis using motor current signature analysis and the artificial neural network," *International Journal on advanced science Engineering Information Technology*, vol. 10, 2020.
- [34] Mosavi, A.; Salimi, M.; Ardabili, S.F.; Rabczuk, T.; Shamshirband, S.; Varkonyi-Koczy, A. State of the Art of Machine Learning Models in Energy Systems, a Systematic Review. *Energies* 2019, 12, 1301.

- [35] Y. Cheng, "Forecast on Short-Term Wind Speed and Wind Farm Power Generation," in 2015 4th National Conference on Electrical, Electronics, and Computer Engineering, 2015: Atlantis Press, pp. 80-86.
- [36] S. Nunnari, L. Fortuna, and A. Gallo, "Wind time series modeling for power turbine forecasting," *Int. J. Electr. Energy*, vol. 2, pp. 112-118, 2014.
- [37] D. Deepa, S. C. Mana, and A. Sivasangari, "Wind Speed Forecasting Using Machine Learning Models," *Mathematical Statistician and Engineering Applications*, vol. 71, no. 3s2, pp. 36-46, 2022.
- [38] M. Elsaraiti and A. Merabet, "A comparative analysis of the arima and lstm predictive models and their effectiveness for predicting wind speed," *Energies*, vol. 14, no. 20, p. 6782, 2021.
- [39] S. A. Shamsnia, N. Shahidi, A. Liaghat, A. Sarraf, and S. F. Vahdat, "Modeling of weather parameters using stochastic methods (ARIMA model)(case study: Abadeh Region, Iran)," in International Conference on Environment and Industrial Innovation, IPCBEE, 2011, vol. 12.
- [40] S. A. Kale and R. N. Varma, "Aerodynamic design of a horizontal axis micro wind turbine blade using NACA 4412 profile," *International Journal of Renewable Energy Research*, vol. 4, no. 1, pp. 69-72, 2014.
- [41] O. Rajad, M. Hamid, and A. El Marjani, "Fiber orientation effect on the behavior of the composite materials of the horizontal axis wind turbine blade (HAWTB)," in 2018 6th International Renewable and Sustainable Energy Conference (IRSEC), 2018: IEEE, pp. 1-6.
- [42] M. Tarfaoui, O. R. Shah, and M. Nachtane, "Design and optimization of composite offshore wind turbine blades," *Journal of Energy Resources Technology*, vol. 141, no. 5, 2019.
- [43] F. A. Abdulla, K. L. Hamid, A. A. F. Ogaili, and M. A. Abdulrazzaq, "Experimental study of Wear Rate Behavior for Composite Materials under Hygrothermal Effect," in IOP Conference Series: Materials Science and Engineering, 2020, vol. 928, no. 2: IOP Publishing, p. 022009.
- [44] F. A. Abdulla, M. Qasim, and A. A. F. Ogaili, "Influence Eggshells powder additive on thermal stress of fiberglass/polyester composite tubes," in IOP Conference Series: Earth and Environmental Science, 2021, vol. 877, no. 1: IOP Publishing, p. 012039.
- [45] A. A. F. Ogaili, F. A. Abdulla, M. N. M. Al-Sabbagh, and R. R. Waheeb, "Prediction of Mechanical, Thermal and Electrical Properties of Wool/Glass Fiber based Hybrid Composites," in IOP Conference Series: Materials Science and Engineering, 2020, vol. 928, no. 2: IOP Publishing, p. 022004.
- [46] Z. K. Hamdan, A. A. F. Ogaili, and F. A. Abdulla, "Study the electrical, thermal behaviour of (glass/jute) fibre hybrid composite material," in *Journal of Physics: Conference Series*, 2021, vol. 1783, no. 1: IOP Publishing, p. 012070.
- [47] M. Hamzah and A. Gatta, "Design of a novel carbon-fiber ankle-foot prosthetic using finite element modeling," in IOP Conference Series: Materials Science and Engineering, 2018, vol. 433, no. 1: IOP Publishing, p. 012056
- [48] E. S. Al-Ameen, J. J. Abdulhameed, F. A. Abdulla, A. A. F. Ogaili, and M. N. M. Al-Sabbagh, "Strength characteristics of polyester filled with recycled GFRP waste," *J. Mech. Eng. Res*, vol. 43, pp.178-85,2020.
- [49] A. A. F. Ogaili, E. S. Al-Ameen, M. S. Kadhim, and M. N. Mustafa, "Evaluation of mechanical and electrical properties of GFRP composite strengthened with hybrid nanomaterial fillers," *AIMS Materials Science*, vol. 7, no. 1, pp. 93-102, 2020.
- [50] Z. Hashin and A. Rotem, "A fatigue failure criterion for fiber reinforced materials," *Journal of composite materials*, vol. 7, no. 4, pp. 448-464, 1973.
- [51] Z. Hashin, "Failure criteria for unidirectional fiber composites," *Journal of Applied Mechanics* vol. 47, no. 2, pp.329-334
- [52] M. Nachtane, M. Tarfaoui, A. El Moumen, and D. Saifaoui, "Damage prediction of horizontal axis marine current turbines under hydrodynamic, hydrostatic and impacts loads," *Composite Structures*, vol. 170, pp. 146-157, 2017.
- [53] P. A. Kulkarni, W. Hu, A. S. Dhoble, and P. M. Padole, "Statistical wind prediction and fatigue analysis for horizontal-axis wind turbine composite material blade under dynamic loads," *Advances in Mechanical Engineering*, vol. 9, no. 9, p. 1687814017724088, 2017.
- [54] M. Hoffmann, R. Reuss Ramsay, and G. Gregorek, "Effects of grit roughness and pitch oscillations on the NACA 4415 airfoil," *National Renewable Energy Lab.(NREL), Golden, CO (United States); The Ohio ...*, 1996.
- [55] D. Salimi-Majd, V. Azimzadeh, and B. Mohammadi, "Loading analysis of composite wind turbine blade for fatigue life prediction of adhesively bonded root joint," *Applied Composite Materials*, vol. 22, no. 3, pp. 269-287, 2015.
- [56] P. A. Kulkarni, A. S. Dhoble, and P. M. Padole, "Deep neural network-based wind speed forecasting and fatigue analysis of a large composite wind turbine blade," *Proceedings of the Institution of Mechanical Engineers, Part C: Journal of Mechanical Engineering Science*, vol. 233, no. 8, pp. 2794-2812, 2019, doi:10.1177/0954406218797972.
- [57] E. S. Al-Ameen, F. A. Abdulla, and A. A. F. Ogaili, "Effect of Nano TiO₂ on Static Fracture Toughness of Fiberglass/Epoxy Composite Materials in Hot Climate regions," in IOP Conference Series: Materials Science and

Engineering, 2020, vol. 870, no. 1: IOP Publishing, p. 012170.

Table of Acronyms

Acronyms	Meaning
machine learning	ML
Finite Element Analysis	FEA
wind turbine blades	WTBs
Autoregressive Integrated Moving Average	ARIMA
Root Mean Square Error, and	RMSE
Mean Absolute Percentage Error	MAPE
Mean Absolute Error	MAE
Akaike information Criterion	AIC
BayesianInformation Criterion	BIC
Glass-fiber-reinforced polymer	GFRP
HSNFTCRT	Fibertensile initiation criterion
HSNFCCRT	Fiber compressive initiation criterion.
HSNMTCRT	Matrix tensile initiation criterion.
HSNMCCRT	Matrix compressive initiation criterion